Scientific
Research
Publishing

Effect of SrO on the Structure of Apatite and Wollastonite Phases of Na$_2$O-CaO-SiO$_2$-P$_2$O$_5$ Glass System

Gomaa El Damrawi[1]*, Rawya Mhammed Ramadan[2], Mohamed El Baiomy[1]

[1]Glass Research Group, Physics Department, Faculty of Science, Mansoura University, Mansoura, Egypt
[2]Microwave Physics and Dielectrics Department, Physics Research Division, National Research Centre, Cairo, Egypt
Email: *gomaaeldamrawi@gmail.com

Abstract

Glasses in the system 24.5Na$_2$O·24.5CaO·6P$_2$O$_5$·xSrO·(45−x)SiO$_2$ have been studied in the composition region of x = 0 - 15 mol%. The as prepared glasses are transparent and have an amorphous network structure. On the other hand, heat treated glasses are transformed to opaque white glass ceramic characterized by their highly crystalline network structure. Crystalline apatite (calcium phosphate, Ca$_3$(PO$_4$)$_2$, wollastonite (calcium silicate, CaSiO$_3$), and strontium calcium phosphate Ca$_2$Sr(PO$_4$)$_2$ are the main well-formed crystalline species played the major role in material bioactivity. Increasing SrO leads to enhancing material crystallite and enhances the hardness of the host glass matrix. The change of XRD spectra, ^{31}P NMR chemical shift and hardness number upon increasing SrO are considered due to modification of the apatit Ca(PO$_3$)$_2$ to involve Sr ions inducing Ca$_2$Sr (PO$_4$)$_2$ apatite one. Such species play the role in enhancing material properties and hardness.

Keywords

Structure, Physical Properties, Gasses, Glass Ceramics

1. Introduction

Porous inorganic materials have unique properties which are useful for the development of biomaterials to become eligible for controlled loading stresses and/or release of biologically active substances [1] [2]. Specifically, the term bioactive glasses or glass ceramics is only applied on any compatible material that can form a calcium phosphate interfacial layer resembles to the biological apatite presents in bones [3] [4]. In addition, bioactive glasses can actively stimulate bone growth through the release of critical concentrations of ionic dissolution products that

cause rapid expression of genes regulating osteogenesis and the production of growth factors [1] [5]. In this regard, strontium-based bioactive glasses have the great ability to inhibit bone resorption by osteoclasts [6] [7]. It was recently demonstrated that SrO enhances the surface adhesion properties for strontium-containing glasses leading to the increasing in material hardness. The enhancement of surface adhesion is considered to be due to the lower electronegativity of Sr compared with that of Ca^{2+} ions in the glassy network [8] [9]. The low electronegativity of Sr leads also to the formation of more stable Si O Sr bond due to a more balanced distribution of electronic charges. The well-formed Ca-P species would be more quickly changed into an apatite layer and more Ca^{2+} substitutions are made possible within the newly formed apatite layer for Sr-doped glasses [10].

The strontium oxide-doped glasses in the SiO_2-CaO-SrO and SiO_2-CaO-P_2O_5-SrO systems have been studied [11] [12]. The interaction processes of the bioactive glasses with biological fluids was determined and it was found that the strontium containing glasses have a good potential for the formation of bone-like apatite [13] [14] [15]. Bioactivity of glasses is usually correlated to exchange of alkali (Na) or alkaline (Ca^{2+}) earth ions with H^+ of the solution. This process leads to condensation of silanols groups ($\equiv$Si-OH) which is an important function that readily reacts with hydroxyl groups, carboxylic acids, and oxides present on inorganic compounds. In such a case, the surface is characterized with its high area. This silica gel layer offers or provides a large number of sites required for formation and growth of hydroxycarbonate apatite species equivalent to the mineral phase of bone [16].

The transition from the highly bioactive glass to biocompatible compositions is characterized by a marked increase in the connectivity of the silicate network through bonding with Sr cations and by the increasing the fraction of phosphate groups involved as P-O-Si or P-O-Sr cross-links. Our analysis also highlights a possible correlation between the enhancement of crystalline apatite through aggregation between Ca^{2+} and PO_4^{3-} ions to form an apatite crystals structure which may be precipitated on the $CaSiO_3$ as a wallsotinte crystalline phases. In this situation, the process of thermal heat treatment is applied as an effective route for crystallization enhancement [17] [18].

2. Materials and Methods

2.1. Sample Preparation

An ordinary dissolve quenching technique was used to produce amorphous glasses within the system $xSrO$-$(45-x)SiO_2$-$24.5CaO$-$24.5Na_2O$-$6P_2O_5$, (0×15 mol %). Samples are obtained from reagent grade mixtures $CaCO_3$, Na_2CO_3, SiO_2, $SrCO_3$, and $(NH_4)_2HPO_4$ which have been melted in a Pt-Au crucible. To remove NH_3 and H_2O, The specimens were heat treated at a slow rate of 2°/min from room temperature to 600°C, then melted for 20 - 30 minutes between 1000°C and 1200°C before being quenched by pouring the melt between two metallic plates. To re-

strict P_2O_5 volatilization and keep total glass weight losses under 2%, the time of melting and temperatures were optimized.

2.2. Infrared Spectra (IR)

The FTIR absorption spectroscopy for different samples were carried out by means of KBr pellets technique .The spectra are measured in the region of 400 - 4000 cm^{-1} with a spectral resolution of 2 cm using a Mattson 5000 FTIR spectrometer. The obtained spectrum was normalized to the spectrum of blank KBr pellet and were corrected to the background and dark currents using two-point baseline correction. The normalization is necessary to eliminate the concentration effect of the powder sample in the KBr disc.

2.3. X-Ray Diffraction Spectroscopy

Shimadzu X-ray diffract meter is used for X-ray diffraction measurements (the apparatus type Dx-30, Metallurgy institute, El Tebbin-Cairo). The values of the maximum peak and intensity are used to determine the material type that compared to patterns in the joint committee for powder diffraction standards' international powder diffraction file (PDF) database (JCPDS).

2.4. Differential Scanning Calorimetry

A NETZSCH STA 409C/CD instrument was used to perform the DSC analysis. Crushed samples of known mass (30 mg) were put in an aluminum tray, sealed with a crimped lid, and heated at a rate of 5˚C/min with argon as the carrier gas at a flow rate of 30 cm^3/min from 25˚C to 1000˚C.

2.5. Heat Treatment (HT)

The samples containing 0, 3, 5, 10 and 15 mol% SrO, were heated in a muffle furnace (Heraeus KR170) controlled within ±2˚C. The samples were heat-treated at temperatures 500˚C and 650˚C for treatment time interval of 6 hours. After heating, the glasses were then kept into the furnace and held at the temperature of heat treatment for the desired time before cooling normally at room temperature.

2.6. Density and Molar Volume

The densities of the prepared samples were calculated using the Archimedes principle and benzene as the immersion solvent. The density was determined using the following formula:

$$\rho = \frac{W_a}{W_a - W_b} \times \rho_b \tag{1}$$

where, W_a is the weight in air, W_b is the weight in benzene, and ρ_b is the density of benzene.

The molar volumes (V_m) were numerically determined using the equation that follows:

$$V_m = \frac{M_T}{\rho} \qquad (2)$$

where V_m is the molar volume. M_T is the glass sample's molecular weight and ρ is the sample's density.

2.7. Micro Hardness

The hardness value (H_v) of the prepared samples was determined using the SHI-MADZU-HMV-G20S (Shimadzu, Kyoto, Japan) micro hardness tester at room temperature Ten indentations have been loaded at different places on the surface. The corresponding length of the indentation imprint diagonals registered by a high resolution microscope to ensure the accuracy of the measurement. The formula was used to calibrate the microhardness (H_v) values:

$$H_V = 1.854 \frac{F}{d^2} \qquad (3)$$

where H_v is the Vickers hardness in kg/mm^2, F is the applied force in newtons, and d is the indentation's mean diagonal length in meters.

2.8. Magnetic Resonance Measurements

The JEOL GSX-500 high-resolution solid state MAS NMR spectrometer with a magnetic field of 11.74 T was used to analyses fine powdered samples of various compositions (Mansoura University-EGYPT). ^{31}P MAS NMR experiments were also conducted at resonance frequency (202.4 MHz) using a 3.2 mm diameter rotor spinning at 15 kHz. Solid NH4H2PO4 was used as a secondary reference compound and the signal from this set to 0.9 ppm. A pulse length of 2.5 μs and a recycle delay of 5 s was applied.

3. Results and Discussion

SrO gives the glasses good advantages toward improvements of their properties like extremely high resistant to thermal shock, high mechanical strength, good chemical stability, crystallinity and bioactivity [19]. It is evidenced from x-ray diffraction (XRD) and FTIR Figure 1, Figure 2, of the as-prepared glasses that the well-formed structural species are constructed in its amorphous state [8] [21]. The addition of SrO at expense of SiO₂ has no effect on the material structure, since the amorphous structure is the most dominant type, see Figure 1, Figure 2. From these figures, the spectral features do not changes upon increasing SrO contents. Because the glass composition has a limited effect, the thermal heat treatment processes can be applied as an alternative to change the material structure.

Figure 3 shows differential scanning calometr (DSC) curves from which both glass transition (T_g) and crystallization temperatures (T_C) can be determined. The crystallization temperature was ranged between 650°C and 700°C as is shown from Figure 3. In addition, T_g is around 550°C. According to DSC data, the glasses in the present study were all treated thermally at 500°C and 650°C for

6 hours. For example, treating the glass which contains 15 mol% SrO at 500˚C (curve b) can activate the nucleation process that leads to crystallization (curve c) when the glass treated at higher temperature (650˚C), see **Figure 4**. The samples in such a case are simply crystallized which means that transformation into a more ordered structure occurred under the effect of thermal heat treatment and partially depends on the glass composition.
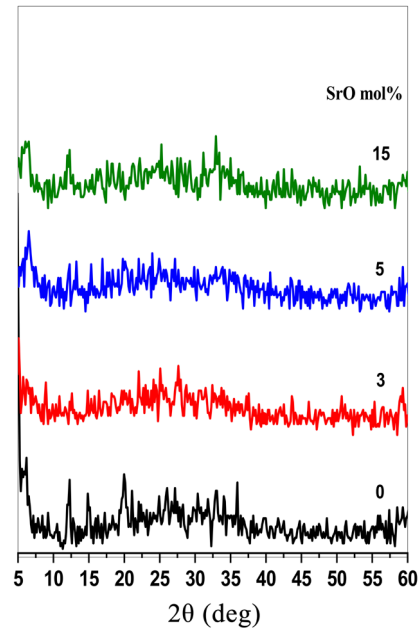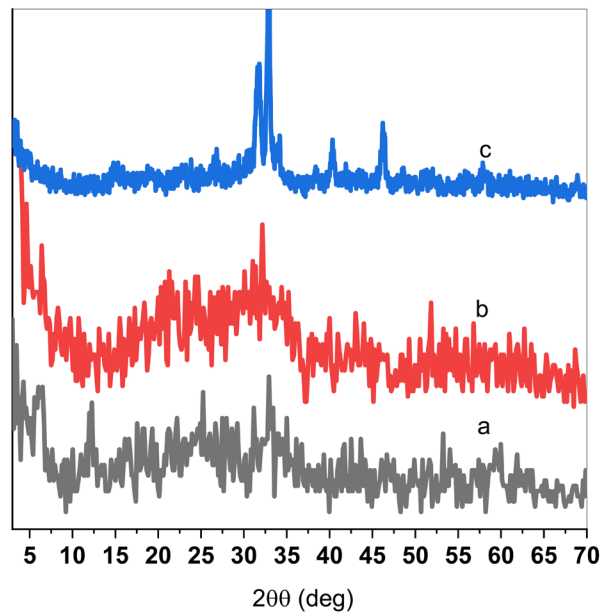

Figure 1. XRD spectra for as prepared glasses containing 0, 5, 10 and 15 mol% SrO.
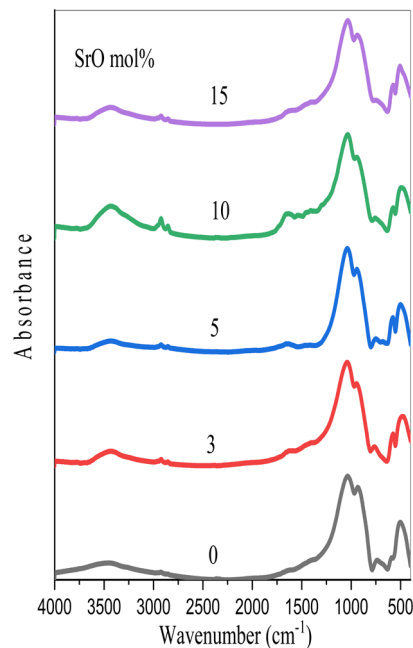
Figure 2. FTIR spectra for as prepared glasses containing 0, 5, 10 and 15 mol% SrO.
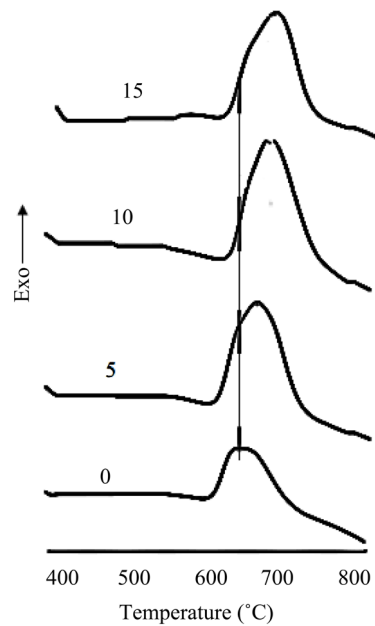
**Figure 3.** DSC micrograph for sample containing 0, 5, 10 and 15 mol% SrO.

Figure 4. XRD for sample containing 5 mol% SrO, (a) as prepared, (b) treated at 500°C treated and (c) trated at 650°C for 6 hours.

Comparisons of the studied materials' X-ray sharp diffraction line spectra with that of apatite ($Ca_3(PO_4)_2$) wollastonite ($CaSiO_3$) and [$Ca_2Sr(PO_4)_2$) crystals were considered. The most developed crystalline species are calcium phosphate, calcium silicate, and calcium strontium phosphate, according to the comparison [20]. The crystalline apatite and wollstonite formed species are considered the main units which play the role of biocompatibility and or bioactivity of the studied materials [21] [22]. **Figure 1**, **Figure 4**, and **Figure 5** of the XRD spectra

indicate that the crystallization process is only available by thermal treatment. The number of diffraction lines in all investigating glasses is the same, but the most noticeable parameter is the change in intensities. This means that the well-formed crystalline phase types remain the same, but the content of the separated phases increases as SrO concentrations rise. Some well-formed crystalline phases, such as crystalline apatite (calcium phosphate crystals) and strontium calcium phosphate, are classified as bioactive phases that are beneficial to dental materials [23] [24].

There is a clear difference between the FTIR spectra of as prepared abd treated samples, **Figure 2** and **Figure 5**. The low frequency peaks between 400 and 600 al showed splitting in case of thermal treating cases. Such splitting in the absorption peaks lent support that both apatite and the wollastonite are formed in its crystalline phases. Which is confirmed by XRD **Figure 5**. Then, in general, SrO in the matrix of the heat treated glasses modifies the silicate and phosphate structural units, forming wollastonite-apatite crystal phases and $Ca_2Sr(PO_4)_2$ apatite microcrystals [card no. 52-0467]. The latter type is more chemically stable against acid and fluid attack when it applied as a cements for oral applications.

Then from the above discussions, we conclude that increasing SrO leads to enhancing material crystallite of the treated glasses which in most cases enhances the mechanical properties. **Figure 6** shows the dependence of the hardness nimbler of the glasses on SrO content. Increasing the amounts of SrO enhances the hardness of the glasses which is changed from 280 kg/mm² to 450 Kg/mm².
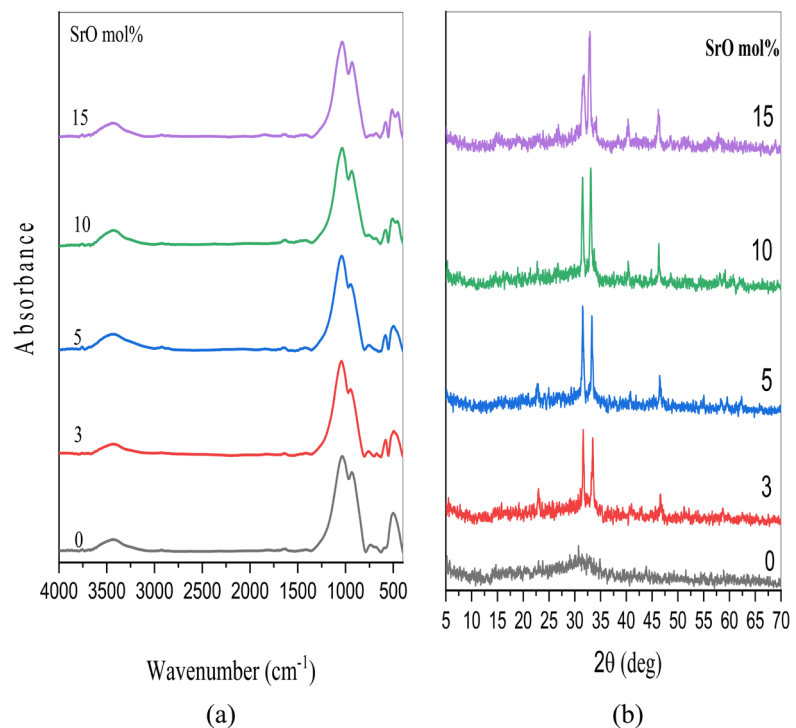
Figure 5. (a) XRD & (b) FTIR for sample containing different concentrations from SrO trated at 650°C for 6 hours.
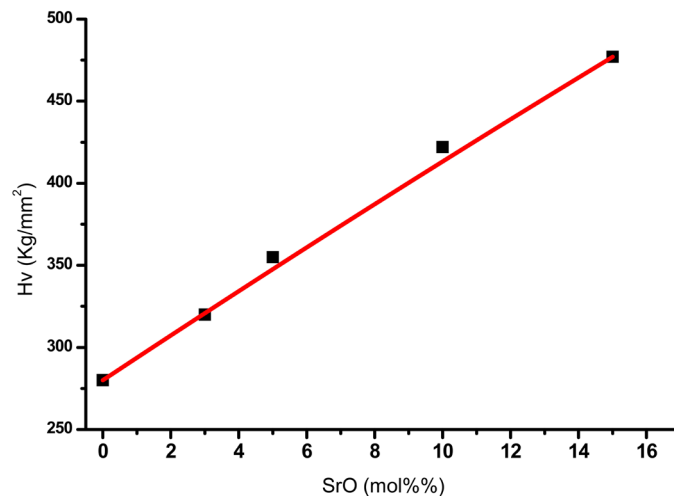
Figure 6. Change of hardness for sample containing different concentrations from SrO trated at 650°C for 6 hours.

The change of XRD spectra and hardness number upon increasing SrO are considered due to modification of the apatit $Ca(PO_3)_2$ to involve Sr ions inducing $Ca_2Sr(PO_4)_2$ apatite one. Such species play the role in enhancing material hardness.

3.1. NMR Measurements

Figure 7 presents ^{31}P NMR spectra of different glasses containing 0, 5 and 15 mol% SrO which were all treated thermally at 650 for 6 hours. The phosphate units of Q^0 species (all oxygens are nonbridging) have been found in the main glass network indicating that the majority of phosphorus exists as orthophosphate species in the glass (Na_3PO_4 or $Ca_3(PO_4)_2$ or mixing between them) [25]. The change of the relative area of three spectra with SrO confirms the above consideration, since the relative area under the ^{31}PNMR spectra is increased by increasing SrO content that means that some of SrO my be forced to enter the apatite phase forming stransium apatie one. Then the apatite crystall shoud be formed from mixed cation (Ca and Sr) instesd of the one type (Ca) presnted by the lower area in **Figure 7**.

The clear difference between 23 NMR spectra of glasses of 0 and 15 mol SrO **Figure 8** support the vesion that Sr can substiute both Na or Ca from the apatite phase and some of Sr can shair in performing the apatite crystalline phases. From **Figure 8**, the chemical shift of Na nuclei of the glasses containing Sr is lower than that of Sr free glass. This means that bond strength in network structure of glasses containing Sr is stronger than that of Sr free ones.
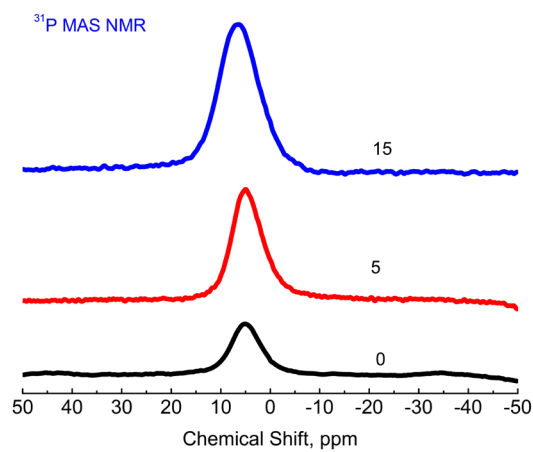
3.2. Density and Molar Volume Measurements

Changes of both density (*D*) and molar volume (*V_m*) with increasing SrO concentration are presented in **Figure 9**. The density increased and its molar volume decreased as the content of SrO is increased from 0 to 15 mol%. The observed icreased in density values is mainly due to higher molecular weight of

SrO (103.62 g/mol) when it compared with that of SiO_2 (60.09 g/mol). Accordingly, with increasing SrO content, SrO enters gradually the network as a glass forming species which leads to increasing the total bridging bonds at the expense of non-bridging ones (Sr-O-Si). As a consequence, formation of shortening Sr-O-P linkages is considered the main reason for the well-decreased volume of the network structure. The decreasing in NBO is accompanied with decreasing the open volume and void spaces surrounded NBO ions which in all cases results in decreasing the molar volume of the studied glass.

SrO (mol%)	Total area (cm²)
0	33
5	64
15	95

Figure 7. ^{31}P NMR spectra for glasses containing different SrO concentration and treated at 650 for 6 hours.
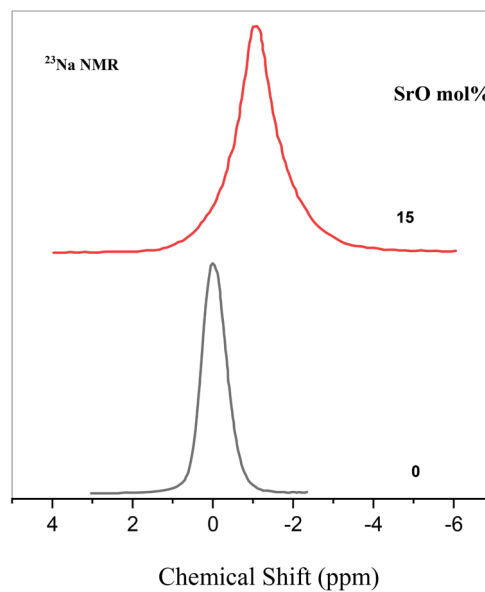
Figure 8. ^{23}Na NMR spectra for glasses containing different SrO concentration.
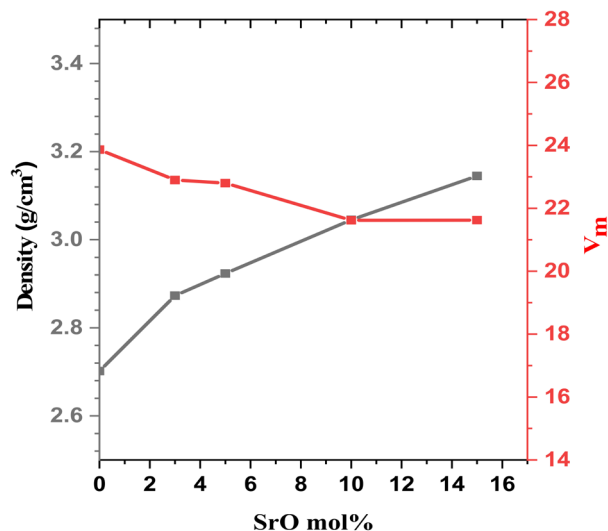
Figure 9. The Density and molar volume as function of SrO content (mol %).

4. Conclusion

Bioglasses and glass ceramics containing different SrO concentrations have been studied by different structural techniques. Amorphous nature of the glass free from SrO is confirmed by XRD. Some types of crystalline species are formed in SrO containing glasses after heat treatment. Well-formed apatite ($Ca_3(PO_4)_2$), wollastonite ($CaSiO_3$) and [$Ca_2Sr (PO_4)_2$] phases containing strontium ions are evidenced in SrO containing glasses. More enhancement in crystallinity was confirmed via thermal heat treatment process. Presence of Sr ions in both crystalline apatite and wollastonite matrix promotes its biocompatibility, particularly orthopedic bioactivity.

Conflicts of Interest

The authors declare no conflicts of interest regarding the publication of this paper.

References

[1] Lao, J., Nedelec, J.-M. and Jallot, E. (2009) New Strontium-Based Bioactive Glasses: Physicochemical Reactivity and Delivering Capability of Biologically Active Dissolution Products. *Journal of Materials Chemistry*, **19**, 2940-2949. https://doi.org/10.1039/b822214b

[2] Ogueri, K.S., Jafari, T., Ivirico, J.L.E. and Laurencin, C.T. (2019) Polymeric Biomaterials for Scaffold-Based Bone Regenerative Engineering. *Regenerative Engineering and Translational Medicine*, **5**, 128-154. https://doi.org/10.1007/s40883-018-0072-0

[3] Kaur, G., Pandey, O.P., Singh, K., *et al.* (2014) A Review of Bioactive Glasses: Their Structure, Properties, Fabrication and Apatite Formation. *Journal of Biomedical Materials Research Part A*, **102**, 254-274.

[4] Fernandes, H.R., Gaddam, A., Rebelo, A., *et al.* (2018) Bioactive Glasses and Glass-Ceramics for Healthcare Applications in Bone Regeneration and Tissue Engineering.

Materials, **11**, 2530. https://doi.org/10.3390/ma11122530

[5]   O'Neill, E., Awale, G., Daneshmandi, L., *et al.* (2018) The Roles of Ions on Bone Regeneration. *Drug Discovery Today*, **23**, 879-890.
https://doi.org/10.1016/j.drudis.2018.01.049

[6]   Lao, J., Jallot, E. and Nedelec, J.-M. (2008) Strontium-Delivering Glasses with Enhanced Bioactivity: A New Biomaterial for Antiosteoporotic Applications? *Chemistry of Materials*, **20**, 4969-4973. https://doi.org/10.1021/cm800993s

[7]   Zhou, Y., Wu, C. and Chang, J. (2019) Bioceramics to Regulate Stem Cells and Their Microenvironment for Tissue Regeneration. *Materials Today*, **24**, 41-56.
https://doi.org/10.1016/j.mattod.2018.07.016

[8]   Al-Qaysi, M. (2018) Development of Phosphate Based Glass Scaffolds for the Repair of Craniofacial Bone. UCL (University College London), London.

[9]   Deshmukh, K., Kovářík, T., Křenek, T., *et al.* (2020) Recent Advances and Future Perspectives of Sol-Gel Derived Porous Bioactive Glasses: A Review. *RSC Advances*, **10**, 33782-33835. https://doi.org/10.1039/D0RA04287K

[10] Bee, S.-L. and Abdul Hamid, Z.A. (2020) Hydroxyapatite Derived from Food Industry Bio-Wastes: Syntheses, Properties and Its Potential Multifunctional Applications. *Ceramics International*, **46**, 17149-17175.
https://doi.org/10.1016/j.ceramint.2020.04.103

[11] Salman, S.M., Salama, S.N. and Abo-Mosallam, H.A. (2012) The Role of Strontium and Potassium on Crystallization and Bioactivity of Na_2O-CaO-P_2O_5-SiO_2 Glasses. *Ceramics International*, **38**, 55-63. https://doi.org/10.1016/j.ceramint.2011.06.037

[12] Massera, J. and Hupa, L. (2014) Influence of SrO Substitution for CaO on the Properties of Bioactive Glass S53P4. *Journal of Materials Science: Materials in Medicine*, **25**, 657-668. https://doi.org/10.1007/s10856-013-5120-1

[13] Wu, C., Zhou, Y., Lin, C., *et al.* (2012) Strontium-Containing Mesoporous Bioactive Glass Scaffolds with Improved Osteogenic/Cementogenic Differentiation of Periodontal Ligament Cells for Periodontal Tissue Engineering. *Acta Biomaterialia*, **8**, 3805-3815. https://doi.org/10.1016/j.actbio.2012.06.023

[14] Zhang, J., Zhao, S., Zhu, Y., *et al.* (2014) Three-Dimensional Printing of Strontium-Containing Mesoporous Bioactive Glass Scaffolds for Bone Regeneration. *Acta Biomaterialia*, **10**, 2269-2281. https://doi.org/10.1016/j.actbio.2014.01.001

[15] Kargozar, S., Lotfibakhshaiesh, N., Ai, J., *et al.* (2016) Synthesis, Physico-Chemical and Biological Characterization of Strontium and Cobalt Substituted Bioactive Glasses for Bone Tissue Engineering. *Journal of Non-Crystalline Solids*, **449**, 133-140.
https://doi.org/10.1016/j.jnoncrysol.2016.07.025

[16] Erasmus, E.P.-I. (2017) Synthesis, Testing and Characterization of Porous Biocompatible Porous Bioactive Glasses for Clinical Use. PhD Dissertation.

[17] Brauer, D.S. (2015) Bioactive Glasses—Structure and Properties. *Angewandte Chemie International Edition*, **54**, 4160-4181. https://doi.org/10.1002/anie.201405310

[18] Eckert, H. (2018) Structural Characterization of Bioactive Glasses by Solid State NMR. *Journal of Sol-Gel Science and Technology*, **88**, 263-295.
https://doi.org/10.1007/s10971-018-4795-7

[19] Mysen, B.O. and Richet, P. (2018) Silicate Glasses and Melts. Elsevier.

[20] Duminis, T., Shahid, S. and Hill, R.G. (2017) Apatite Glass-Ceramics: A Review. *Frontiers in Materials*, **3**, 59. https://doi.org/10.3389/fmats.2016.00059

[21] El-Damrawi, G., Hassan, A.K., Kamal, H., Aboelez, M. and Labeeb, S. (2016) Structural Investigations on Na_2O-CaO-V_2O_5-SiO_2 Bioglass Ceramics. *British Journal of*

Applied Science and Technology, **16**, 1-9.
https://doi.org/10.9734/BJAST/2016/26683

[22] Kenny, S.M. and Buggy, M. (2003) Bone Cements and Fillers: A Review. *Journal of Materials Science: Materials in Medicine*, **14**, 923-938.
https://doi.org/10.1023/A:1026394530192

[23] Gómez-Morales, J., Iafisco, M., Delgado-López, J.M., Sarda, S. and Drouet, C. (2013) Progress on the Preparation of Nanocrystalline Apatites and Surface Characterization: Overview of Fundamental and Applied Aspects. *Progress in Crystal Growth and Characterization of Materials*, **59**, 1-46.
https://doi.org/10.1016/j.pcrysgrow.2012.11.001

[24] Irfan, M. and Irfan, M. (2020) Overview of Hydroxyapatite; Composition, Structure, Synthesis Methods and Its Biomedical Uses. *Biomedical Letters*, **6**, 17-22.

[25] Ahmed, I., Parsons, A.J., Rudd, C.D., *et al.* (2008) Comparison of Phosphate-Based Glasses in the Range $50P_2O_5\text{-}(50-x)$ CaO-xNa$_2$O Prepared Using Different Precursors. *Glass Technology—European Journal of Glass Science and Technology Part A*, **49**, 63-72.